Available online at www.sciencedirect.com
ScienceDirect
Journal of Photochemistry and Photobiology A: Chemistry 186 (2007) 85–92
Journal of Photochemistry and Photobiology A:Chemistry
www.elsevier.com/locate/jphotochem

Synthesis, spectral properties and photostability of novel boron–dipyrromethene dyes

Aijun Cui, Xiaojun Peng *, Jiangli Fan, Xiuying Chen, Yunkou Wu, Binchen Guo

State Key Laboratory of Fine Chemicals, Dalian University of Technology, 158 Zhongshan Road, Dalian 116012, PR China

Received 6 March 2006; received in revised form 24 May 2006; accepted 27 July 2006
Available online 5 August 2006

Abstract

Two series of novel boron–dipyrromethene (BODIPY) dyes containing 8-phenyl groups have been synthesized and their spectral properties have been studied. Series **2** with four methyl groups at 1,3,5,7-positions show much higher fluorescence quantum yields and extinction coefficients than series **1** (without methyl groups). The "push–pull" electronic effect caused by the methyl groups at 3 and 5 positions is a significant positive factor to the high quantum yields of **2**. The X-ray structure analysis of **1c** and **2c** reveals that steric expulsion exists between the phenyl and adjacent two methyl groups. Moreover, the steric expulsion might block the intramolecular vibronic relaxation and internal conversion of the excited **2**, which also contributes to their high fluorescence quantum yields. The substituent effects on photostability and redox potentials of these dyes have been discussed.

Keywords: Boron–dipyrromethene dye; Crystal structure; Fluorescence quantum yield; Photostability; Cyclovoltammetry; Intramolecular vibronic relaxation; Internal conversion

1. Introduction

In the past few years, there have been a lot of boron–dipyrromethene (BODIPY) dyes' innovations [1,2]. This kind of dyes is comparatively easy to be oxidized and reduced, which triggers BODIPY fluorophores' application in photoswitches based on the theory of electron or charge transfer (CT) [3,4]. Generally, the BODIPY fluorophores present advantageous photo-spectral properties, such as high extinction coefficients and high fluorescence quantum yields [5], which facilitate their applications in DNA sequencing and bio-analysis [6–8].

However, various substituents at BODIPY framework may lead to large difference on their spectral properties, especially on the quantum yields. Vos de Wael et al. reported that the position and number of alkyl groups modulated the quantum yields from 0.3 to 0.8 [9]. Lindsey et al. found that the BODIPY dyes exhibited considerably smaller emission yields (0.05) after a phenyl was introduced at 8-position [10]. Electronic effect of those substitutents could be contributed to the difference of quantum yields. Steric effect on the fluorescence of BODIPY dyes, however, has not been reported. In this report, by analyzing the distinction of two typical X-ray crystal structures, we describe a kind of steric effect that is proved to be one of the important factors on quantum yields of BODIPY dyes in some cases.

The photostability is one of the fatal properties of BODIPY dyes for their practical applications, especially in electrogenerated chemiluminescence and laser irradiating [11–13]. It is surprising that only a few papers concern the photodegradation of BODIPY dyes [14,15] and the relationship between photostability and the substituents at the skeleton of BODIPY dyes is unclear. In this article, the substituent effects (Fig. 1) on the photostability are checked and discussed.

2. Experiment

2.1. Characteristics of the dyes

The single-crystal X-ray data were collected on a Siemens SMART CCD diffractometer. ^{1}H NMR spectra were recorded on a VARIAN 400 MHz NMR spectrometer. Electronic absorption spectra were obtained on a HP-8453 spectrophotometer.

* Corresponding author. Tel.: +86 411 88993899; fax: +86 411 88993906.
E-mail address: pengxj@dlut.edu.cn (X. Peng).

1010-6030/$ – see front matter © 2006 Elsevier B.V. All rights reserved.
doi:10.1016/j.jphotochem.2006.07.015

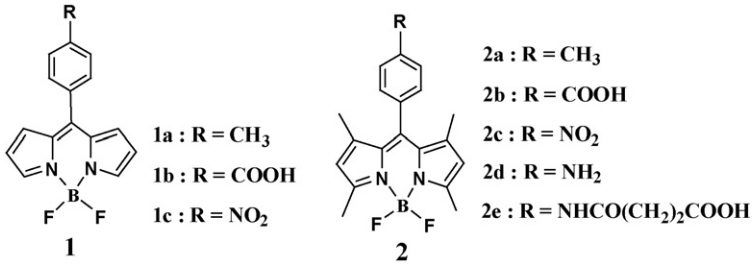

Fig. 1. Structures of two series of BODIPYdyes.

Fluorescence measurements were performed on a PTI-C-700 Felix and Time-Master system. HRMS data were obtained on MICROMASS HPLC-Q-TOF MS system. The redox potential was measured on BAS 100B electorchemical analyzer. A three-electrode cell was composed of a glass carbon as working electrode, a platinum wire as counter electrode, and Ag/Ag+ as reference electrode (0.01 M $AgNO_3$). The supporting electrolyte was $TBAPF_6$ (0.1 M tetra-*n*-butylammonium hexafluorophosphate) and the concentration of the dyes was 10^{-3} M in CH_3CN. All the chemicals used for the experiments were of analytical grade.

The corresponding fluorescence quantum yields were calculated according to a standard solution of fluorescein (from Aldrich Company) in 0.1 M NaOH ($\Phi = 0.85$) and was determined using the model [16]:

$$\Phi_x = \Phi_s \left(\frac{A_s}{A_x}\right)\left(\frac{F_x}{F_s}\right)\left(\frac{n_x}{n_s}\right)^2$$

where Φ is the fluorescence quantum yield, A is the absorbance, F is the area under the emission curve, and n is the refractive index of the solvents used in measurement. The subscript s and x represent the standard dye (fluorescein) and the tested dye, respectively.

2.2. Photofading

The photofading was carried out in quartz cells (1 cm in width) where sample solution was irradiated with a 500 W *I–W* lamp at room temperature. In order to eliminate the heat and the absorbance of short wavelength light, a cold trap (10 L solution of 50 g/L $NaNO_2$ and 20 cm in length) was set up between the cells and the lamp. The distance between the cells and the lamp was 25 cm. The irreversible bleaching of the dyes at the absorption peak was monitored as a function of time. All the dyes' toluene solutions were deoxygenated with argon.

2.3. Synthesis

Series dyes **1** were prepared from pyrrole and *p*-substituent benzaldehyde in a one-pot reaction [17]. General procedure: 4.5 mmol of pyrrole and 2 mmol of the aldehyde were dissolved in 150 mL of absolute methylene chloride under argon atmosphere. One drop of trifluoroacetic acid was added and the solution was stirred at room temperature until TLC-control showed complete consumption of the aldehyde. At this point, a solution of 2 mmol dichlorodicyanobenzoquinone (DDQ) in CH_2C1_2 was added, and stirring was continued for 10 min followed by addition of 4 mL of triethylamine and 4 mL of BF_3Et_20 quickly. After stirring for another 2 h the reaction mixture was washed with water and dried, and the solvent was evaporated. The residue was chromatographed twice on a silica column (the mixture of CH_2C1_2 and Hexane as eluted solvent). Recrystallization from ethyl acetate/hexane yielded analytically pure samples.

la: total yield: 25%. Orange crystals. ^{1}H NMR ($CDC1_3$): δ 2.479 (s, 3H, CH_3), 6.537 (d, 2H, $J = 10$ Hz, CH), 6.964 (d, 2H, $J = 10$ Hz, CH), 7.345 (d, 2H, $J = 19$ Hz, phenyl), 7.485 (d, 2H, $J = 20$ Hz, phenyl), 7.930 (s, 2H, CH). MS (ESI), *m/z*: 305.3 $[M + Na]^+$. Q-TOFMS: $[M + Na]^+$ calculated: 305.1038, measured: 305.1023.

lb: total yield: 18%. Orange crystals. ^{1}H NMR ($CDC1_3$): δ 6.584 (d, 2H, $J = 8$ Hz, CH), 6.907 (d, 2H, $J = 9$ Hz, CH), 7.707 (d, 2H, $J = 20$ Hz, phenyl), 7.987 (s, 2H, CH), 8.294 (d, 2H, $J = 20$ Hz, phenyl). MS (APCI), *m/z*: 311.1 $[M - H]^-$ Q-TOFMS: $[M - H]^-$ calculated: 311.0918, measured: 311.0945.

lc: total yield: 30%. Red crystals. ^{1}H NMR ($CDC1_3$): δ 6.602 (d, 2H, $J = 9$Hz, CH), 6.855 (d, 2H, $J = 9$Hz, CH), 7.773 (d, 2H, $J = 22$Hz, phenyl), 8.007 (s, 2H, CH), 8.423 (d, 2H, $J = 22$ Hz, phenyl). MS (ESI), *m/z*: 312.0$[M - H]^-$ Q-TOFMS: $[M - H]^-$ calculated: 312.0870, measured: 312.0842.

The synthesis of **2a**–**2c** was similar to that of series dyes **1**, but the pyrrole was changed into 2,4-dimethylpyrrole. **2a**: total yield: 35%. Orange crystals.^{1}H NMR ($CDC1_3$): δ 1.394 (s, 6H, CH_3), 2.462(s, 3H, CH_3), 2.546 (s, 6H, CH_3), 5.964 (s, 2H, CH), 7.144 (d, 2H, CH $J = 19$Hz), 7.286 (d, 2H, *CYU* = 19Hz). ^{13}C NMR (400 MHz, $CDC1_3$): 155.385, 143.354, 142.337, 138.989, 132.112, 131.778, 129.949, 127.937, 121.250, 21.574, 14.720, 14.599. MS (ESI), *m/z*: 361.3 $[M + Na]^+$. Q-TOFMS: $[M + Na]^+$calculated: 361.1664, measured: 561.1647.

2b: total yield: 26%. Orange crystals. ^{1}H NMR ($CDC1_3$): δ 1.373 (s, 6H, CH_3), 2.566 (s, 6H, CH_3), 6.001 (s, 2H, CH), 7.464 (d, 2H, CH $J = 20$ Hz), 8.250 (d, 2H, CH $J = 20$ Hz). MS (APCI), *m/z*: 367.5 $[M - H]^-$ Q-TOFMS: $[M - H]^-$ calculated: 567.1544, measured: 567.1512.

2c: total yield: 48%. Orange crystals. ^{1}H NMR ($CDC1_3$): δ 1.363 (s, 6H, CH_3), 2.567 (s, 6H, CH_3), 6.017 (s, 2H, CH), 7.554 (d, 2H, *CHJ* = 21 Hz), 8.401 (d, 2H, *CHJ* = 22 Hz). MS (ESI), *m/z*: 368.2 $[M - H]^-$ Q-TOFMS: $[M - H]^-$ calculated: 368.1496, measured: 568.1472.

The reduction of **2c**: 1 mmol **2c** and 0.5 mL NH_2NH_2–H_2O were added in 50 mL ethanol with 10 mg Pd/C as catalyst under argon atmosphere. After reflux for 2 h, TLC-control showed complete consumption of the **2c**, and a new product appeared. Then the reaction system was cooled to room temperature, and the catalyst and the solvent were removed. The residue was chromatographed on a silica column eluted with CH_2Cl_2/hexane 2:1. **2d**: total yield: 96%. Orange solid (this compound is easy to be oxidized, and its color will turn to red). ^{1}H NMR ($CDC1_3$): δ 1.556 (s, 6H, CH_3), 2.545 (s, 6H, CH_3), 5.969 (s, 2H, CH), 6.854 (d, 2H, CH J = 20 Hz), 7.054 (d, 2H, CH.J = 20 Hz). MS (ESI), m/z: 340.3 $[M+H]^+$. Q-TOFMS: $[M+H]^+$calculated: 340.1752, measured: 340.1781.

2e can be synthesized by acidylation of **2d** with succinic anhydride, 1 mmol **2d** and 1.1 mmol succinic anhydride were dissolved in 20 mL CH_3CN under argon atmosphere, and the mixture was refluxed for about 10 h. TLC-control showed complete consumption of the **2d**, and then the solvent was removed. The residue was chromatographed on a silica column eluted with CH_2Cl_2/hexane/methanol 100:50:0.5. **2e**: total yield: 65%. Orange solid. ^{1}H NMR ($CDC1_3$): δ 1.398 (s, 6H, CH_3), 2.444 (s, 6H, CH_3), 2.560 (d, 2H, CH_2 J = 5 Hz), 2.610 (d, 2H, CH_2 J = 6 Hz), 6.175 (s, 2H, CH), 7.281 (d, 2H, CH J = 21 Hz), 7.797 (d, 2H, CH J = 21 Hz). MS (ESI), m/z: 438.3 $[M-H]^-$. Q-TOFMS: $[M-H]^-$ calculated: 438.1915, measured: 438.1936.

3. Result and discussion

3.1. Synthesis of BODIPY dyes

As is shown in Scheme 1, BODIPY dyes are synthesized in the one-pot reactions: in the first step, dipyrrolemethanes are prepared by the condensation of benzenealdehydes and pyrroles; the second step requires dichlorodicyanobenzoquinone (DDQ) for the oxidation of dipyrrolemethenes; and finally, $BF_3{\cdot}Et_2O$ is employed to coordinate with nitrogen atom. The total synthetic yields are related to the substituents of benzenealdehydes and pyrroles. For the *p*-substituents at benzenealdehyde, the electron-withdrawing groups (such as NO_2, **1c**: 30%; **2c**: 48%) are beneficial to get higher yields than the electron-donating group (CH_3, **1a**: 25%; **2a**: 35%). The electron withdrawing groups may enhance the activity of benzenealdehyde

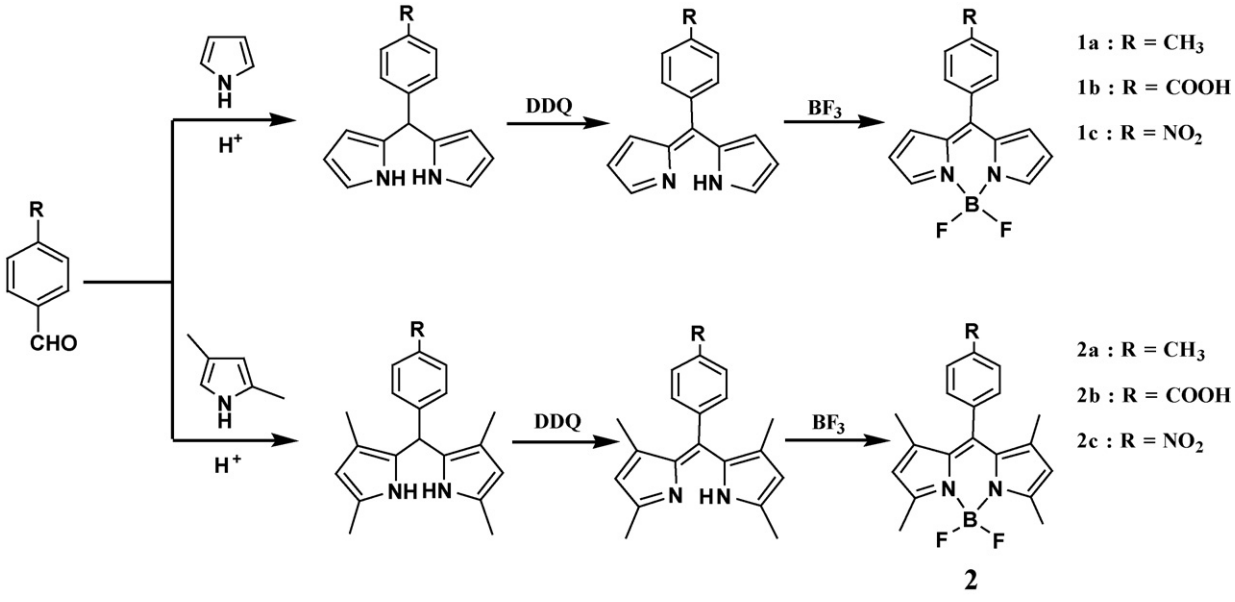

Scheme 1. Synthetic routes of **1** and **2** (**a**–**c**).

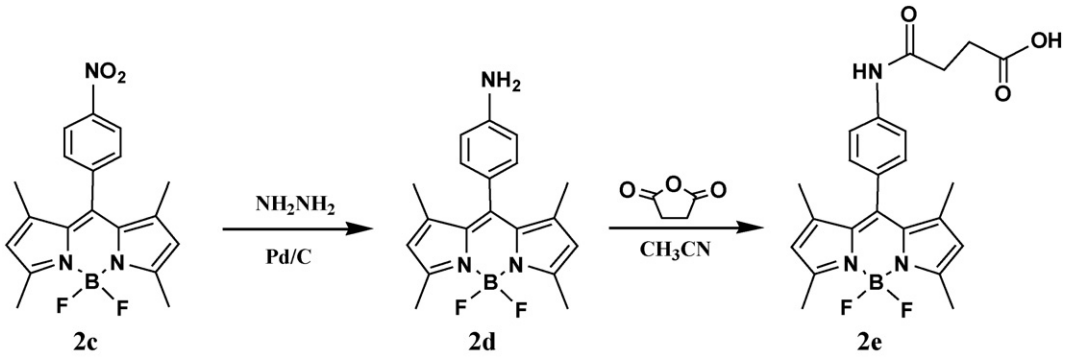

Scheme 2. Synthetic routes of derivatives (**2d**–**e**) from **2c**.

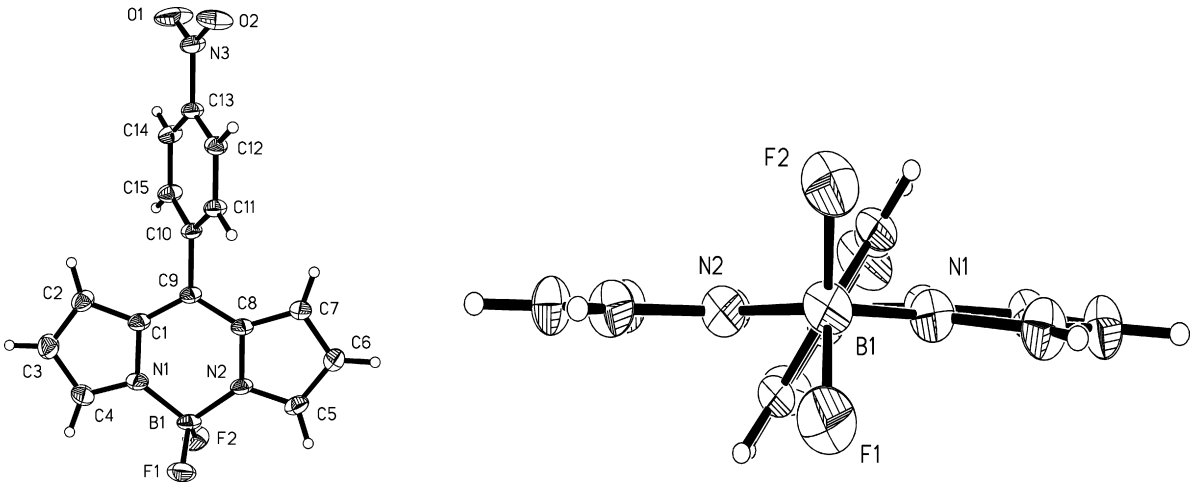

Fig. 2. X-ray structure of compound **1c**.

in the electrophilic addition reactions. On the other hand, 2,4-dimethylpyrrole is more reactive with the aldehydes than pyrrole, thus series dyes 2 (**2a**: 35%; **2b**: 28%; **2c**: 48%) are with higher yields than series **1(1a:** 25%; **1b**: 18%; **1c**: 30%). From **2c**, **2d** and **2e** can be obtained by reduction and succinoylation sequentially (Scheme 2).

3.2. Crystal structure of *1*c and *2c*

From the mixture solution of CH_2Cl_2–hexane (3:1) at 5 °C, single crystals of **1c** and **2c** were obtained (Figs. 2 and 3). Up to now, very limited single crystals of BODIPY dyes have been prepared, and these two crystals will be helpful to revealing the relation between the dyes' structures and their properties. The X-ray outcome of **1c** (Fig. 2) shows that the BODIPY framework is almost a plane, and the dihedral-angle between the phenyl and BODIPY plane is about 56°. The plane defined by F–B–F atoms is perpendicular with that of BODIPY skeleton, similar to the previous reports [18]. In the crystal structure of **2c**, the dihedral-angle between the phenyl and BODIPY plane is 78° (Fig. 3), which is obviously different from that in **1c**. The distinction of the dihedral-angles may influence many physical properties of these two series dyes. The crystallographic data, selected bond distances and angles are showed in Tables 1 and 2.

3.3. Spectral properties of dyes

As is listed in Table 3, the absorption maxima ($\lambda_{max(ab)}$) of the two series dyes are about 500 nm, and show only a little substituent effects (<6 nm). The fluorescent spectra, however, red shift by 23 nm in ($\lambda_{max(em)}$) from **1a** to **1c** and 29 nm from **2a** to **2c** in methylene dichloride, and Stokes shifts ($\Delta\lambda$) increase to 35 nm. It is noticeable that the extinction coefficients (ε) of **2** are much larger than those of **1**, and **2** have narrower spectra and smaller Stokes shifts than **1** (Fig. 4). It might be the result of the "push–pull" electronic effect of methyl groups of **2**.

The most remarkable differences of the dyes in emission are their fluorescent quantum yields (Φ_f). As nitro-group is a well-known quenching group of fluorescence, **1c** and **2c** have rather low quantum yields ($\Phi_f < 0.02$). The Φ_f of **2a** and **2b**, however, are almost 10 times larger than those of the corresponding **1a** and **1b**. The different macroscopical physical properties of molecules are inevitably related to their microcosmic structures.

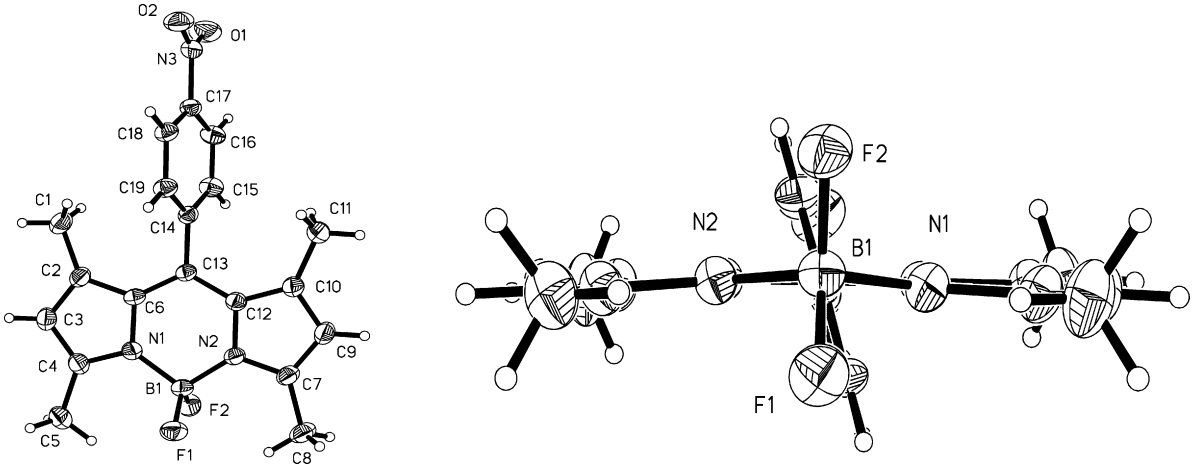

Fig. 3. X-ray structure of compound **2c**.

Table 1
Crystallographic data for **1c** and **2c**

	Compound	
	1c	**2c**
Crystal system	Triclinic	Monoclinic
Space group	*P*-1	*C*2/*c*
a (Å)	7.8605(3)	30.5729(6)
b (Å)	8.0103(3)	11.8625(2)
c (Å)	11.4271(5)	19.8975(5)
α (°)	89.093(2)	90.00
β (°)	85.4180(10)	96.7320(10)
γ (°)	72.5540(10)	90.00
V (Å^{-3})	684.19(5)	7166.5(3)
Z	2	16
$D_{calc.}$ (mg m^{-3})	1.520	1.369
μ (Mo Kα), (m^{-1})	0.120	0.103
F (0 0 0)	320	3072
Crystal size (mm^3)	0.21 × 0.25 × 0.30	0.41 × 0.45 × 0.52
2θ range	1.79–25.12	1.34–25.04
Index ranges	$-9 \le h \le 8, -5 \le k \le 9, -13 \le l \le 12$	$-30 \le h \le 36, -7 \le k \le 14, -19 \le l \le 23$
Reflections collected	2185	4790
Unique data/ restraints/ parameters	2372/0/209	6278/0/678
R_f, R_w	0.0711, 0.2064	0.0858, 0.1898
Largest remaining peak/hole (e Å^{-3})	0.368/−0.365	0.316/−0.272

Table 3
Spectra properties of **1** and **2** in dichloromethane and ethanol

Dyes	Solvent	$\lambda_{max(ab)}$ (nm)	$\lambda_{max(em)}$ (nm)	$\Delta\lambda$ (nm)	ε 10^5 (M^{-1} cm^{-1})	Φ_f
1a	CH_2C1_2	500	521	21	0.61	0.051
	Ethanol	498	518	20	0.60	0.034
lb	CH_2C1_2	505	525	20	0.62	0.026
	Ethanol	500	522	22	0.64	0.031
1c	CH_2C1_2	509	544	35	0.66	0.010
	Ethanol	506	541	35	0.67	0.0082
2a	CH_2C1_2	500	510	10	0.97	0.60
	Ethanol	499	508	9	1.1	0.61
2b	CH_2C1_2	503	516	13	1.2	0.57
	Ethanol	500	509	9	1.2	0.59
2c	CH_2C1_2	506	539	32	1.4	0.020
	Ethanol	503	529	26	1.3	0.017
2d	CH_2C1_2	500	514	14	1.3	0.31
	Ethanol	498	516	18	1.2	0.014
2e	CH_2C1_2	502	512	10	1.1	0.53
	Ethanol	499	509	10	1.2	0.57

As is shown in Fig. 5, the methyl groups in BODIPY skeleton may enhance electronic "push–pull" effect and also increase the fluorescence quantum yields of dyes as in the case of **2a**, **3**, **4** and **5**. The fluorescence quantum yield of **5** is 0.38 with two methyl groups at 3 and 5 positions [19], which is much larger than that of **1a** (without methyl groups, $\Phi_f = 0.034$). It implies that 3- and 5-methyl groups have a positive effect on Φ_f. This phenomenon is due to the electronic "push–pull" effect of the two methyl groups on BODIPY fluorophore. On the other hand, dye 3 and dye 4 have different number of methyl groups but almost the same high fluorescence quantum yields (Φ_f: 0.81 and 0.80, respectively) [9], it is noticeable that the electronic effect of the methyl groups at 1 and 7 positions is ignorable for the quantum yields of dyes. However, the electronic effect can not rationally explain the result that the quantum yield of **2a** (Φ_f: 0.61) is still higher than **5** (Φ_f: 0.38). Steric effect might be the other factor.

The crystal structures of **1c** and **2c** are helpful to revealing this steric effect. X-ray analysis of the crystals shows that the most important distinction between **1** (or **5**) and **2** series dyes is the dihedral angles between phenyl and BODIPY plane, which are about 56° and 78°, respectively. The steric exclusion between

Table 2
Selected bond distances and angles in **lc**, **2c**

1c				**2c**			
Bond distance (Å)		Angle (°)		Bond distance (Å)		Angle (°)	
B–F1	1.379(3)	F1–B–F2	108.5(2)	B–F1	1.385(5)	F1–B–F2	109.4(4)
B–F2	1.382(3)	F1–B–N1	110.6(2)	B–F2	1.385(5)	F1–B–Nl	110.5(4)
B–N1	1.542(4)	F1–B–N2	111.0(2)	B–N1	1.543(6)	F1–B–N2	110.6(4)
B–N2	1.538(4)	B–N1–C1	125.7(2)	B–N2	1.540(6)	B–N1–C4	125.9(4)
Nl–C1	1.394(3)	B–N1–C4	127.2(2)	N1–C4	1.346(6)	B–N1–C6	125.8(3)
N1–C4	1.336(4)	B–N2–C5	126.5(2)	N1–C6	1.400(5)	B–N2–C7	126.6(3)
N2–C5	1.339(4)	B–N2–C8	126.3(2)	N2–C7	1.357(5)	B–N2–C12	125.4(3)
N2–C8	1.393(3)	N1–B–N2	106.06(19)	N2–C12	1.407(5)	N1–B–N2	106.9(3)
N3–O1	1.207(3)	N1–C1–C9	120.6(2)	N3–O1	1.226(5)	N1–C6–C2	108.0(4)
N3–O2	1.211(3)	N1–C1–C2	107.6(2)	N3–O2	1.219(5)	N2–C12–C13	120.0(4)
N3–C13	1.471(3)	N2–C8–C9	120.1(2)	N3–C17	1.480(5)	C4–N1–C6	108.1(3)
C1–C2	1.411(4)	N2–C8–C7	107.7(2)	C2–C3	1.376(6)	C6–C13–C12	121.4(4)
C1–C9	1.390(3)	C1–C9–C10	120.0(2)	C2–C6	1.431(6)	C6–C13–C14	119.3(3)
C2–C3	1.360(4)	C1–C9–C8	120.7(2)	C3–C4	1.406(6)	C7–N2–C12	108.0(3)
C3–C4	1.394(5)	C1–N1–C4	107.1(2)	C6–C13	1.404(6)	C12–C13–C14	119.3(4)
C8–C9	1.400(4)	C5–N2–C8	107.1(2)	C12–C13	1.404(5)	C13–C14–C19	120.4(4)
C9–C10	1.486(3)	C8–C9–C10	119.3(2)	C13–C14	1.491(5)	C13–C14–C15	120.4(4)

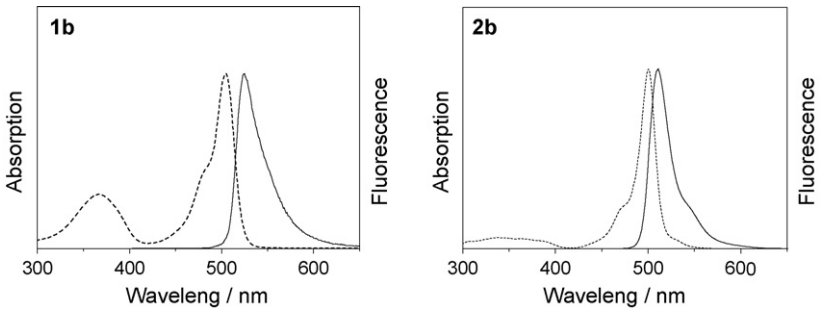

Fig. 4. Absorption (dash) and emission (solid) spectra of **1b**(left) and **2b**(right) in dichloromethane.

8-phenyl group and 1, 7-methyl groups in **2** series dyes strengthens the phenyl plane's tendency of being perpendicular to the BODIPY plane, while the phenyl plane in **1** or **5** is rather free as no such steric exclusion exists. When the dyes are excited, the free phenyl group is easy to quench emission and increase the efficiency of internal conversion (IC) via intramolecular vibronic relaxation. Blocking the vibration or rotation of the phenyl group by 1-and 7-methyl groups in **2** can suppress the IC process [20,21], which is the significant reason that **2** presents higher fluorescence quantum yields than **5** and **1**. Therefore, both the electronic "push–pull" effect and the steric effect result in the distinct quantum yields of **1** and **2** dyes.

Different from **2a** and **2b**, **2d** (with an amino group) shows low fluorescence quantum yields, especially in strong polar solvent, such as ethanol (Φ_f: 0.014). After the amino group is acidylated, **2e** is insensitive to solvent and recovers good quantum yields (Φ_f: 0.53–0.57) sequentially. This means that a PET (photo-induced electronic transfer) process occurs between the amino group and the BODIPY platform in the dye **2d**, and the acidylation of amino can inhibit the effect drastically. [22].

3.4. Photostability of dyes

High photostability is a very important character for practical applications of fluorescent dyes. BODIPY dyes' photostability

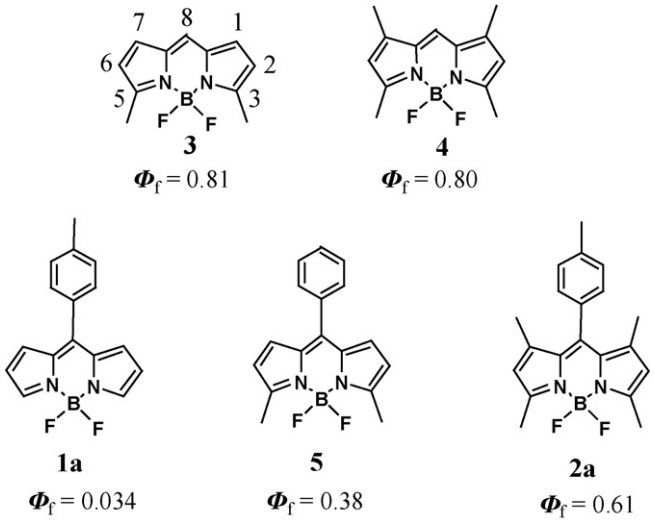

Fig. 5. Five typical BODIPY dyes and their fluorescence quantum yields.

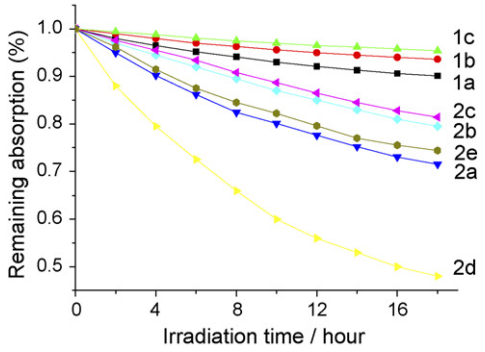

Fig. 6. Comparisons on the photofading of the **1** and **2** dyes in toluene.

is significantly influenced by different substituents. The photofading process of series dyes **1** and **2** were tracked by detecting the decrease of their maximal absorptions in toluene at different times (Fig. 6). Based on Beer rule and the mechanism of photoreaction, the equation of photoreaction is shown as follows [23]:

$$\ln\frac{A_0}{A_t} = kt$$

A_0 is the absorbance in maximal wavelength before the irradiation, and A_t the absorbance in maximal wavelength after the irradiation. The slope, k, is the rate constant of the photofading and listed in Table 4.

It is very clear that dyes **1** are much more stable than dyes **2**. The four methyl groups in dyes **2** will increase the electron cloud density of dye molecules and make dyes **2** easier to be oxidized and less photostable than dyes **1**.

Table 4
The rate constants of photofading and the electrochemical data of dyes in CH_3CN (scan rate 100 mV/s)

Dyes	Rate constants k ($\times 10^{-4}$ mol min^{-1})	E_{ox} (mV)	E_{red} (mV)
1a	0.9652	+1237.5	−1123.0
1b	0.6124	+1276.0	−1081.0
1c	0.4360	+1320.0	−933.0
2a	3.106	+790.0	−1520.5
2b	2.124	+831.0	−1522.5
2c	1.905	+852.0	−1301.5
2d	6.796	+605.5	−1557.0
2e	2.738	+808.5	−1495.0

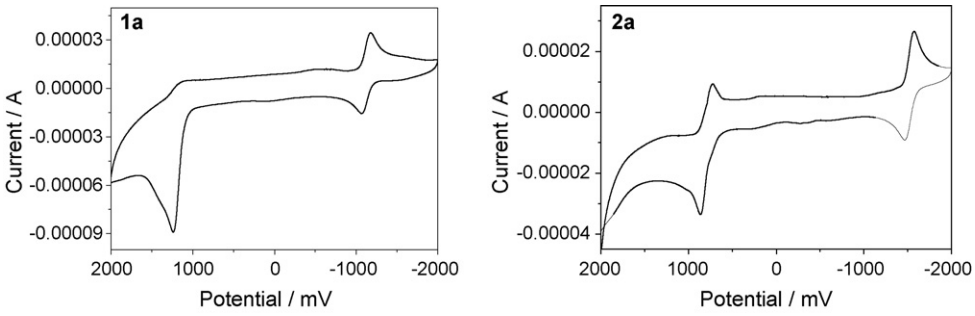

Fig. 7. Cyclic voltammetry curves of the dyes **1a** and **2a** with scan rate of 100 mV/s (vs. Ag/Ag+).

Different *p*-substituent phenyls also affect the photostability of these dyes. When an electron-donating group (such as CH_3, NH_2 or $NHCOCH_2CH_2CO_2H$) is at the *p*-position of phenyl moiety, the photostability will decrease. In contrast, when an electron-withdrawing group (such as COOH, NO_2) is at the *p*-position, the photostability will increase. The amino dye, **2d**, shows the lowest stability; but when the amino group is succinoylated, the photostability of **2e** (with $NHCOCH_2CH_2CO_2H$ group) is as high as **2a**. The terminal COOH in 2e may be activated in the form of succinimide ester and used to label bio-molecules directly [24].

The photostability of these dyes is closely related to their quantum yields. From the data of Fig. 6 and Table 3, a conclusion can be drawn easily that the BODIPY dyes with better photostability generally present lower quantum yields. This may be the result of the synergistic action caused by the electronic "push–pull" effect and the steric effect.

3.5. The relationship between dyes' photostability and their electrochemical properties

In fact, the reaction of photodegradation is a process where a dye is oxidized by singlet oxygen [25]. So the dye's photostability must be related to redox potential. The electrochemical data of dyes are shown in Table 4. The redox potentials of dyes **1** are much higher than those of dyes **2**: the oxidation and reduction potentials of series **2** are more than 1237 mV and −1123.0 mV respectively; while those of series **1** are less than 852 and 1301 mV. This suggests that dyes **1** are harder to be oxidized than dyes **2**. On the other hand, the different *p*-substituents at phenyl group also affect the redox potentials: the electron-donating groups reduce the redox potentials, while the electron-withdrawing groups increase the redox potentials (Table 4). The high oxidation potential is beneficial to the enhancement of photostability.

The cyclic voltammetry curves of **1a** and **2a** (Fig. 7) shows that the oxidation of dyes **2** is reversible, whereas that of dyes **1** is irreversible. The electrochemical polymerization of pyrroles may be related to the irreversible oxidation [26]. The dyes **2** with four methyl groups around BODIPY skeleton are more difficult to polymerize than series dyes **1** because the methyl groups block this process by space repulsion.

4. Conclusion

In summary, we have synthesized two series of BODIPY dyes (**1** and **2**) and researched their spectral properties. Dyes **2** with four methyl groups show much higher fluorescence quantum yields and extinction coefficients than dyes **1**. The X-ray structure analysis of the crystals of **1c** and **2c** is used to reveal that blocking the rotation of 8-phenyl moiety by 1- and 7-methyl groups will suppress the intramolecular vibronic relaxation and internal conversion. The "push–pull" electronic effect caused by methyl groups at 3- and 5-position of BODIPY is another positive factor for the high quantum yields of **2**. The photostability of dyes **1** are higher than that of dyes **2**, and the electron withdrawing *p*-substituents at phenyl moiety of the dyes are beneficial to increasing the photostability. The BODIPY dyes with better photostability present comparatively lower quantum yields in our research.

Acknowledgements

This work was financially supported by the Education Ministry of China and the National Natural Science Foundation of China (project 20128005, 20376010 and 20472012).

References

[1] J. Chen, A. Burghart, A. Derecskei-Kovacs, K. Burgess, J. Org. Chem. 65 (2000) 2900–2906.
[2] Z. Shen, K. Rurack, H. Uno, M. Spieles, B. Schulz, N. Ono, Chem. Eur. J. 10 (2004) 4853–4871.
[3] K. Rurack, M. Kollmannsberger, U. Resch-Genger, J. Daub, J. Am. Chem. Soc. 122 (2000) 968–969.
[4] C. Trieflinger, K. Rurack, J. Daub, Angew. Chem. Int. Ed. 44 (2005) 2288–2291.
[5] J. Karolin, L. Strandberg, L.B.-A. Johansson, J. Am. Chem. Soc. 116 (1994) 7801–7806.
[6] S.A. Farber, M. Pack, S.Y. Ho, L.D. Johnson, D.S. Wagner, Science 292 (2001) 1385–1388.
[7] F. Bergstrom, L. Mikhalyov, L.B.-A. Johansson, J. Am. Chem. Soc. 124 (2002) 196–204.
[8] A.L. Weiner, A. Lewis, M. Ottolenghi, M. Sheves, J. Am. Chem. Soc. 123 (2001) 6612–6616.
[9] E. Vos de Wael, J.A. Pardoen, J.A. von Koeveringe, J. Lutenburg, Reel. TraV. Chim. Pays-Bas 96 (1977) 306–309.
[10] R.W. Wagner, J.S. Lindsey, Pure Appl. Chem. 68 (1996) 1373–1380.
[11] M. Kollmannsberger, K. Rurack, U. Resch-Genger, J. Daub, J. Phys. Chem. A 102 (1998) 10211–10220.

[12] G. Ulrich, R. Ziessel, J. Org. Chem. 69 (2004) 2070–2083.
[13] T.L. Arbeloa, F.L. Arbeloa, I.L. Arbeloa, Chem. Phys. Lett. 299 (1999) 315–321.
[14] G. Jones II, O. Klueva, S. Kumar, D. Pacheco, Proc. SPIE-Int. Soc. Opt. Eng. 4267 (2001) 24–32.
[15] W.N. Wade, N. Ono, T. Yano, M. Wada, Dyes and Pigments 55 (2002) 143–150.
[16] R.A. Velapoldil, H.H. Temnesenl, J. Fluoresc. 14 (2004) 465–472.
[17] K. Rurack, M. Kollmannsberger, J. Daub, Angew. Chem. Int. Ed. 40 (2001) 385–487.
[18] M. Kollmannsberger, T. Gareis, S.J. Daub, Angew. Chem. Int. Ed. 36 (1997) 1333–1335.
[19] W. Qin, M. Baruah, N. Boens, J. Phys. Chem. A 109 (2005) 7371–7384.
[20] A. Demeter, T. Berces, L. Biczok, J. Phys. Chem. 100 (1996) 2001–2011.
[21] F. Li, S.I. Yang, J.S. Lindsey, J. Am. Chem. Soc. 120 (1998) 10001–10017.
[22] F. Song, X. Peng, E. Lu, Tetrahedron Lett. 46 (2005) 4817–4820.
[23] C. Ping, S. Shuqing, H. Yunfeng, Q. Zhiguo, Z. Deshui, Dyes Pigm. 41 (1999) 227–231.
[24] H. Maas, G. Calzaferri, Angew. Chem. Int. Ed. 41 (2002) 2284–2288.
[25] M.A.J. Rodgers, J. Am. Chem. Soc. 105 (1983) 6201–6205.
[26] R.Y. Lai, A.J. Bard, J. Phys. Chem. B 107 (2003) 5036–5042.